

Sensitivity and resilience of the climate system: A conditional nonlinear optimization approach



H.A. Dijkstra*, J.P. Viebahn

Institute for Marine and Atmospheric research Utrecht, Center for Extreme Matter and Emergent Phenomena, Utrecht University, Princetonplein 5, 3584 CC Utrecht, The Netherlands

ARTICLE INFO

Article history:

Received 30 April 2014
Received in revised form 9 July 2014
Accepted 18 September 2014
Available online 15 October 2014

Keywords:

Climate sensitivity
Nonlinear stability
Bifurcation
Resilience

ABSTRACT

In this paper, we propose the concepts of conditional climate resilience and conditional climate sensitivity as measures of the nonlinear response of a non-stationary background climate state to arbitrary perturbations. Based on the theory of nonlinear stability, we formulate both sensitivity and resilience in terms of a conditional nonlinear optimization problem. As illustrated by results of a zero-dimensional energy balance model, the new measures provide useful information of sensitivity and resilience of the climate system in the presence of bifurcations and under non-stationary external forcing.

© 2014 Elsevier B.V. All rights reserved.

1. Introduction

At the moment, the climate system is exposed to a substantial increase in the concentration of atmospheric greenhouse gases. For example, the values of the concentration of carbon dioxide ($p\text{CO}_2$) have increased from 280 ppmv up to about 400 ppmv over the last 150 years [1]. Because the response time scales of the natural carbon-cycle processes on observables such as the global mean temperature are much longer, this greenhouse gas change can be considered as a transient ‘external forcing’ imposed on the climate system [2].

One of the important issues in future climate change is how large the global mean surface temperature, indicated below by T , will become in the year 2100. The concept of equilibrium climate sensitivity S_{eq} (also referred to as Charney sensitivity [3,4]) has been introduced with the aim to provide a scalar measure of the response of the climate system to changes in ‘external forcing’. In practice, it is the equilibrium change in the global mean surface temperature (ΔT) due to a doubling of $p\text{CO}_2$, i.e.,

$$S_{eq} = \frac{\Delta T}{\Delta R} \quad (1)$$

where ΔR is the change in radiative forcing associated with this change in $p\text{CO}_2$. The quantity S_{eq} can be determined from simulations of climate models where ΔT is the temperature change between a control (equilibrium) simulation (under a fixed $p\text{CO}_2$) and an equilibrium simulation under a $2x$ $p\text{CO}_2$ concentration.

The equilibrium climate sensitivity can be connected to the feedbacks in the climate system, such as the ice–albedo feedback and the water–vapor feedback. Some feedbacks operate on time scales shorter or comparable to the change in $p\text{CO}_2$

* Corresponding author.

E-mail addresses: h.a.dijkstra@uu.nl (H.A. Dijkstra), j.p.viebahn@uu.nl (J.P. Viebahn).

while others occur on much longer time scales [5]. When ΔT is considered to be small with respect to the background state temperature, then it can be shown that [6]

$$S_{eq} = \frac{\lambda_0}{1-f} \quad (2)$$

where λ_0 is the ‘pure’ sensitivity (the direct radiative effect) due to pCO₂ changes and f represents the sum of all climate feedbacks. Under the assumption that f is normally distributed, [6] show that S_{eq} has a long tail, in agreement with those found in large-scale ensemble climate simulations (e.g., <http://climateprediction.net>), and suggests that climate sensitivity is difficult to predict. This view has been challenged by Zaliapin and Ghil [7], who point out that the approach by Roe and Baker [6] is only valid for small ΔT . Also the fact that the feedbacks have a normal distribution is challenged as this has not been shown from simulations of general circulation models. With a nonlinear correction as introduced in [7], however, the spectrum of S_{eq} does not match those from <http://climateprediction.net> as good as that of [6].

It has been well-recognized that the concept of equilibrium climate sensitivity is quite limited when making adequate projections of global mean surface temperature for the end of this century [8]. The climate system has a strong internal variability on many time scales, is subject to a non-stationary forcing and certainly out of equilibrium with the changes in the radiative forcing up to the year 2100. Alternative concepts of climate sensitivity have therefore been suggested, for example based on a Fokker–Planck adjoint approach [9], based on Wasserstein distances [8] and based on linear response theory [10]. Here, we will follow another approach by considering the issue of climate sensitivity from a nonlinear stability theory point of view.

The approach is derived from the theory of nonlinear stability of fluid flows [11] and is ideally suited to develop a non-stationary and nonlinear concept of climate sensitivity based on the finite time response of the climate system to a so-called Conditional Nonlinear Optimal Perturbation (CNOP). The CNOP is a so-called finite amplitude perturbation and the response to this perturbation cannot be determined from the linearized equations around the background state but involves the full nonlinear equations. The CNOP [12] methodology has been applied to derive nonlinear stability boundaries in many idealized fluid flows, such as pipe flows [13,14]. It has also been much used to study the predictability of properties in geophysical flows [12,15].

Within the nonlinear stability theory framework, it is also possible to address the issue of resilience of the climate system. Resilience has been much discussed and used in ecosystems and socioeconomic systems and can be generally viewed as the ability of a certain dynamical system to absorb a disturbance and still retain its basic function and structure [16,17]. This is particularly relevant if the climate system would possess more than one equilibrium state under the present-day forcing. If the climate system turns out to be only weakly resilient, finite amplitude perturbations may be able to induce a transition to a very different climate on a finite time scale and the Earth system may drift towards a less inhabitable planet [18].

This paper is organized as follows. In Section 2, the background on nonlinear stability theory and CNOP computation is briefly reviewed and subsequently used to define conditional climate sensitivity and conditional climate resilience. In Section 3, the application of these concepts will be illustrated using the results from a zero-dimensional energy balance model. A discussion of these results and the potential for using the new concepts is provided in Section 4.

2. Sensitivity and resilience: a nonlinear stability theory perspective

In the Section 2.1, we provide an overview of nonlinear stability theory such as developed in [11]. Next, the practical implementation of this theory using Conditional Nonlinear Optimal Perturbation (CNOP) techniques is presented in Section 2.2. Finally, the new concepts of conditional climate sensitivity and conditional climate resilience are introduced in Section 2.3.

2.1. Nonlinear stability theory

In the nonlinear stability theory of fluid flows [11], usually an energy norm E (for example, the kinetic energy) is chosen and a specific basic (or background) state is called asymptotically stable when

$$\lim_{t \rightarrow \infty} \frac{E(t)}{E(0)} = 0 \quad (3)$$

where $E(0)$ is the initial energy of the perturbation and t indicates time. If there exists a positive value δ such that the background state is asymptotically stable only for $E(0) < \delta$, then the basic state is said to be conditionally stable. If $\delta \rightarrow \infty$, then the basic state is called globally stable and if (3) is satisfied and $dE(t)/dt < 0$ holds for all $t > 0$, then the basic state is said to be monotonically stable. Note that this definition of stability does not imply that the perturbations should be small a priori.

Let one of the parameters in a particular model be an important control parameter, e.g. affecting the background state. In fluid flows the control parameter is mostly the Reynolds number [11] which is here indicated by R . According to the notions above, the following possibilities exist (cf. Fig. 1). In region I, the basic state is monotonically stable; all perturbations, whatever their amplitude, have a monotonically decaying energy. In region II, there may be perturbations which initially grow (not necessarily exponentially), but the energy eventually decays to zero for all initial amplitudes of the perturbations. Such

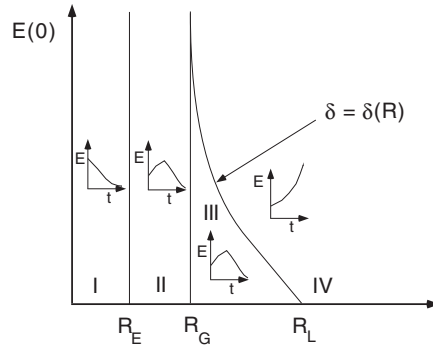


Fig. 1. Plot of the different stability regimes, with I: monotonic stability, II: global stability, III: conditional stability and IV: instability. The control parameter is R and the stability bounds R_E , R_G and R_L are the energy, global and linear stability bounds, respectively. The curve $\delta_c(R)$ bounds the magnitude of the perturbations not leading to a transition; the region of conditional stability is bounded by $R_G < R < R_L$. Typical trajectories of the energy E are sketched to illustrate the different behavior in each domain.

behavior is closely related to non-normal growth phenomena [19] where, due to the non-normality of the linearized operator, a combination of normal modes can lead to algebraic growth of perturbations, even when each of the normal modes has a negative growth factor. Region III is a region of conditional stability, since if the initial amplitude of the perturbations is small enough ($E(0) < \delta_c(R)$) the perturbation energy decays to zero, whereas if it is larger than some particular value $\delta_c(R)$, the energy will increase and the perturbed state will evolve to a different state than the background state. Hence, the latter indicates that the background state is (nonlinearly) unstable to finite amplitude perturbations.

From Fig. 1, stability boundaries can be defined according to the evolution of the perturbation energy E . If $R < R_G$ then the basic state is globally stable, i.e. every perturbation decays to zero in time; R_G is the global stability limit and provides sufficient conditions for stability. If $R < R_E$, the basic state is monotonically stable; R_E is called the energy stability limit. If $R_G < R < R_L$, then the basic state is conditionally stable: small amplitude disturbances decay whereas too large perturbations grow. Beyond the linear stability boundary R_L (i.e. in region IV), infinitesimally small perturbations will grow and this stability bound provides sufficient conditions for instability. Apart from these stability boundaries, also the curve $\delta_c(R)$ is of interest as it provides a measure of the ‘minimal seed’ [13] which is needed to escape from an otherwise linearly stable basic state. The next section deals with the approach to calculate this ‘minimal seed’.

2.2. The Conditional Nonlinear Optimal Perturbation approach

When it is aimed to take nonlinear aspects of the spread of trajectories into account one can resort to optimization methods in which the optimal growth of some norm of the solution is determined. To study nonlinear mechanisms of amplification, Mu [20] proposed the concept of nonlinear singular vectors and nonlinear singular values. In Mu and Duan [12], the concept of the Conditional Nonlinear Optimal Perturbation (CNOP) was introduced (which we shortly discuss in this section) and since then it has been applied to many geophysical flows [21,15]. Alternative computational schemes are presented in [13] but will not be considered here.

After discretization of any spatially extended model of the climate system, a finite dimensional non-autonomous dynamical system of the form

$$\frac{d\mathbf{x}}{dt} = \mathbf{f}(\mathbf{x}, t; \lambda) \quad (4)$$

will result. Here $\mathbf{x} \in \mathbb{R}^n$ is the state vector and $\lambda \in \mathbb{R}$ one of the control parameters. For a chosen initial condition at time $t = t_0$, say $\mathbf{x}(t_0) = \mathbf{x}_0$, a trajectory of this system is given by $\mathbf{x}(t)$ for all $t > t_0$.

The nonlinear stability concept deals with the response of the system to finite amplitude perturbations (i.e. those that are large enough such that nonlinear terms in the equations cannot be neglected). In principle, these perturbations could be on the state vector or on the parameters of the system. However, as a parameter can always be included in the state vector by extending it (for example, for a constant parameter value λ_0 , we can add the equation $d\lambda/dt = 0$ with initial condition $\lambda(0) = \lambda_0$) we only need to consider perturbations on the state vector.

Suppose \mathbf{X} is a (not necessarily steady) background solution of (4) and let $\mathbf{y} = \mathbf{x} - \mathbf{X}$ be the perturbation of this background state. The evolution equations for \mathbf{y} can be written as

$$\frac{d\mathbf{y}}{dt} = \mathbf{f}(\mathbf{X} + \mathbf{y}, t; \lambda) - \mathbf{f}(\mathbf{X}, t; \lambda) = \mathbf{g}(\mathbf{y}, t; \mathbf{X}, \lambda) \quad (5)$$

with initial condition (or initial perturbation) $\mathbf{y}(t_0) = \mathbf{y}_0$. If the initial value problem (5) for fixed λ is well posed, then the nonlinear propagator \mathcal{M} is defined as the evolution operator of (5) which determines the trajectory from t_0 up to a final time t_e . Hence, for fixed $t_e > t_0$,

$$\mathbf{y}(t_e) = \mathcal{M}(\mathbf{y}_0; \mathbf{X})(t_e) \quad (6)$$

provides the final value of \mathbf{y} at $t = t_e$.

For a chosen norm $\|\cdot\|$, the perturbation $\mathbf{y}_{0\delta}$ is called the Conditional Nonlinear Optimal Perturbation (CNOP) with constraint condition $\|\mathbf{y}_0\| \leq \delta$, if and only if [12]

$$J(\mathbf{y}_{0\delta}) = \max_{\|\mathbf{y}_0\| \leq \delta} J(\mathbf{y}_0) \quad (7)$$

where the cost function J is given by

$$J(\mathbf{y}_0) = \|\mathcal{M}(\mathbf{y}_0; \mathbf{X})(t_e)\| \quad (8)$$

In short, the CNOP is that initial condition, under the posed constraint, which maximizes the chosen norm of the state vector during the nonlinear evolution of the system. In principle, the norm of the constraint condition and that of the cost function can be chosen differently [15].

With the CNOP approach, the value of $\delta_c(\lambda)$ (for control parameter λ) as in Fig. 1 can in principle be determined. For any value of λ , one solves the optimization problem (7) for a finite time t_e and increasing values of δ . One then monitors the slope of the cost function with respect to δ and determines for every t_e ,

$$\delta(t_e) = \max_{\delta} \left| \frac{\partial J(\mathbf{y}_{0\delta})}{\partial \delta} \right| \quad (9)$$

where $|\cdot|$ is the absolute value. In the limit $t_e \rightarrow \infty$ (and under the condition that this limit exists) and fixed λ , $\delta(t_e)$ will approach a point on the curve $\delta_c(\lambda)$ because the cost function $J(\mathbf{y}_{0\delta})$ of the CNOP $\mathbf{y}_{0\delta}$ will undergo a sharp increase when δ crosses δ_c (cf. Section 3.2 below).

2.3. Conditional climate sensitivity and resilience

Resilience has often been restricted [17] to autonomous systems with fixed points, i.e., points $\bar{\mathbf{X}}$ for which $\mathbf{f}(\bar{\mathbf{X}}; \lambda) = 0$ in (4). When the initial perturbation on a conditionally stable fixed point $\bar{\mathbf{X}}$ is such that the trajectory crosses the attraction basin of that fixed point, another fixed point is approached asymptotically. Clearly, resilience here is related to the magnitude of the perturbation which can cause this cross-attraction-basin behavior in a certain time t_e .

We define conditional resilience $\mathcal{R}(t_e)$ of a conditionally stable background state \mathbf{X} by

$$\mathcal{R}(t_e) = \frac{\delta(t_e)}{\|\mathbf{X}\|} \quad (10)$$

where $\delta(t_e)$ is defined in (9). This quantity clearly depends on the norm chosen as well as the time scale of the response to the perturbation. If $\delta(t_e)$ is very small with respect to $\|\mathbf{X}\|$ then a relatively small perturbation can induce a transition to a remote attractor and hence the system does not show strong resilience. For $t_e \rightarrow \infty$, this will provide the equilibrium conditional resilience $\mathcal{R}_c = \delta_c / \|\mathbf{X}\|$. In case of two stable fixed points which are separated by a saddle fixed point, the equilibrium conditional resilience of each stable state will be related to the distance (in the chosen norm) between that stable state and the unstable state.

The definition $\mathcal{R}(t_e)$ is, however, not restricted to autonomous dynamical systems with fixed points, but can also be applied in non-autonomous systems with general attractors. Also in the more general case, it measures whether the finite time (t_e) response will lead to similar behavior as near the original background state, or whether new dynamical behavior can be expected.

Whereas climate resilience is a measure of the vulnerability of the climate system by focussing on critical thresholds, sensitivity is actually concerned with the amplitude of the response over a finite time period. Climate sensitivity is a special case of this general notion of sensitivity as it is concerned with the development of only the global mean temperature T [3,4]. Using the CNOP approach, we define the concept of conditional climate sensitivity $S(\delta, t_e)$ of a background climate state (indicated by \bar{T}) as

$$S(\delta, t_e) = \frac{\Delta T(\delta, t_e)}{\Delta R(\delta, t_e)} \quad (11)$$

where $\Delta T(\delta, t_e) = |T(t_e) - \bar{T}|$ is the maximum temperature difference that can occur under the constraint $|T(0) - \bar{T}| < \delta$ (although alternative constraints could be considered) over a time t_e and $\Delta R(\delta, t_e)$ is the change in radiative forcing over the same time interval. Note again that scalar norms are used, but the model to determine it can be very high dimensional (large n in (4)).

In a climate system in which there is a single fixed point for each value of pCO_2 , $S(\delta, t_e)$ is independent of δ (i.e., there is no region of conditional stability) and will approach the equilibrium climate sensitivity S_{eq} in the limit $t_e \rightarrow \infty$. In this limit, ΔT will be precisely the difference between the temperature of the equilibrated states and ΔR the difference in radiative forcing between both states.

3. An illustrative case

In this section, we illustrate the concepts from the previous section by applying them to an idealized energy balance model. The parameters in the model are chosen such that all concepts can be demonstrated, rather than to fit them in a way that ‘most realistic’ model results (compared to present-day observations) are found.

3.1. Energy balance model: formulation

In a typical zero-dimensional model of the Earth system only processes determining the global mean surface temperature T are represented. We will use here an energy balance model of Budyko–Sellers type [22,23] as formulated in [24]. The equation is

$$c_T \frac{dT}{dt} = Q_0(1 - \alpha(T)) + G + A \ln C/C_0 - \sigma \epsilon T^4, \quad (12)$$

where c_T is the thermal inertia (in $\text{J m}^{-2} \text{K}^{-1}$). The first term on the right hand side models the short-wave radiation with Q_0 (in W m^{-2}) being the solar constant divided by four and $\alpha(T)$ the planetary albedo. The term $G + A \ln C/C_0$ (in W m^{-2}) represents the effect of greenhouse gases on the radiation balance, where the constant A controls the equilibrium climate sensitivity of the model and C_0 is a reference carbon dioxide concentration. Finally the last term in Eq. (12) represents the long-wave radiation with σ ($\text{W m}^{-2} \text{K}^{-4}$) being the Stefan–Boltzmann constant and ϵ the emissivity.

To take the effects of land ice on the radiation balance into account, the albedo $\alpha(T)$ is prescribed as [25]

$$\alpha(T) = \alpha_0 H(T_0 - T) + \alpha_1 H(T - T_1) + \left(\alpha_0 + (\alpha_1 - \alpha_0) \frac{T - T_0}{T_1 - T_0} \right) H(T - T_0) H(T_1 - T) \quad (13)$$

where $H(x) = (1 + \tanh(x/\epsilon_H))/2$ is a continuous approximation of the Heaviside function. When the temperature drops below $T = T_0$, the albedo α_0 of an ice surface applies and when T exceeds T_1 , the albedo α_1 of an ocean surface applies. Between T_0 and T_1 , a linear relation between albedo and temperature is assumed. In the results below, we will use the standard values as shown in Table 1.

3.2. Constant C case

When using C as a time-independent control parameter, the bifurcation diagram in which the steady state temperature T is plotted versus C is shown in Fig. 2. A stable ‘ice-covered’ state exists up to $C_{L_1} = 700$ ppmv where the saddle node bifurcation L_1 occurs on the lower branch. The stable upper ‘ice-free’ state exists for values of C larger than $C_{L_2} = 212$ ppmv where the saddle-node bifurcation L_2 on the upper branch occurs. Both branches are connected by an unstable branch, indicated by the dashed curve in Fig. 2. The positions of the saddle-node bifurcations depend strongly on the values of the reference temperatures and reference albedo values in the model.

To illustrate the methodology, we first fix $\bar{C} = 500$ ppmv and determine the CNOPs for different δ under fixed values of t_e . The perturbation on \bar{T} is written as T' and as a norm we choose

$$|T'|^2 = (T - \bar{T})^2 \quad (14)$$

where $\bar{T} = 296.004$ is the equilibrium value at the upper branch in Fig. 2. Hence the constrained optimization problem to be solved becomes (7) with

$$J(T'_{0\delta}) = \max_{|T'| \leq \delta} |\mathcal{M}(T'_0; \bar{T})(t_e)| \quad (15)$$

where again \mathcal{M} is the evolution operator of the model (12) on the perturbation T' with respect to \bar{T} .

In Fig. 3(a), the values of $J(T'_{0\delta})$ are shown as a function of δ for three values of t_e . The values of $|T'_{0\delta}|$ are all equal to δ as the CNOP is located on the boundary of the constraint condition. The results in Fig. 3(a) indicate that one is able to determine the unstable state, here the separatrix of the attraction basins of both stable fixed points as measured by the distance δ_c , by

Table 1
Reference values of the parameters in the energy balance model defined by (12) and (13).

Parameter	Value	Parameter	Value
c_T	$5.0 \times 10^8 \text{ J m}^{-2} \text{K}^{-1}$	Q_0	342 W m^{-2}
ϵ	1.0	σ	$5.67 \times 10^{-8} \text{ W m}^{-2} \text{K}^{-4}$
A	$2.05 \times 10^1 \text{ W m}^{-2}$	G	$1.5 \times 10^2 \text{ W m}^{-2}$
C_0	280 ppmv	α_0	0.7
α_1	0.2	T_0	263 K
T_1	293 K	ϵ_H	0.273 K

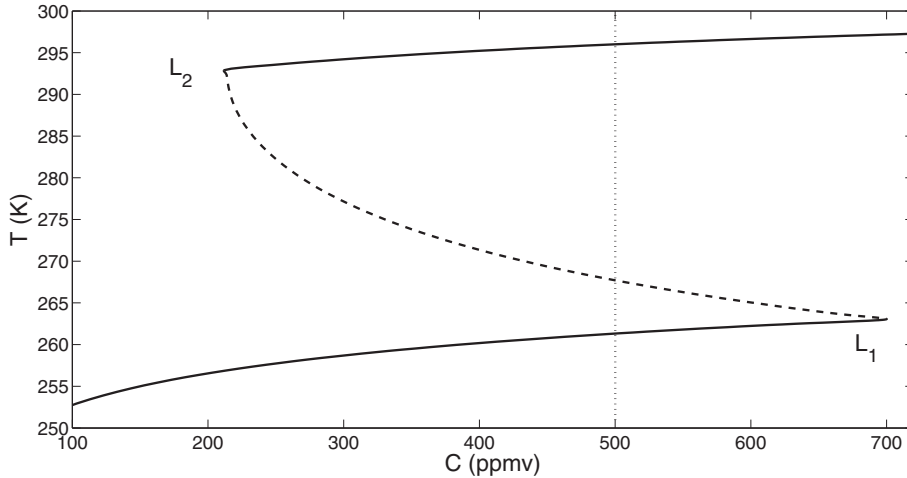


Fig. 2. Bifurcation diagram of the steady state solutions T versus C of the model (12) and (13) with the parameter values as in Table 1.

the CNOP approach. As t_e is increased, a sharp step appears near δ_c as trajectories starting for $|T'_0| < \delta_c$ will end up at the fixed point on the upper branch, whereas those for which $|T'_0| > \delta_c$ will end up on the fixed point on the lower branch. Differentiation of the curves in Fig. 3(a) with respect to δ gives the result in Fig. 3(b) and shows that a maximum in $\gamma = \partial J(T'_{0\delta})/\partial \delta$ occurs for every t_e . The values of $\delta(t_e)$ in (9) are the values of δ for which this maximum is attained and when divided by \bar{T} provides the conditional resilience of the background state $\mathcal{R}(t_e)$ as given in (10); for $t \rightarrow \infty$, the value of $R(t_e) \rightarrow R_c$, where δ_c is given by the difference of the values of T on the upper stable and unstable branch (for $\bar{C} = 500$ ppmv).

In Fig. 4(a) and (b), the conditional resilience $\mathcal{R}(t_e)$ (at three times t_e) is plotted versus C for the background states along the upper (Fig. 4(a)), and lower (Fig. 4(b)) branch of the bifurcation diagram in Fig. 2. The values of R_c are plotted for both branches in Fig. 4(c). From Fig. 4(c) it follows that the equilibrium conditional resilience of the fixed point solutions decreases as the saddle-node bifurcations are approached. Indeed, the attraction domain for the stable fixed point shrinks as the saddle-node bifurcation is approached and hence the amplitude of the perturbation needed to induce a transition decreases. On the upper branch, the conditional resilience can already be determined for small times t_e far from the saddle-node bifurcation L_2 . This is due to fact that for large C , the response time of the system to evolve back to the equilibrium state is relatively small. The conditional resilience is overestimated near the saddle-node bifurcation L_2 and $\mathcal{R}(t_e)$ decreases with t_e . On the lower branch, the opposite behavior is found; the equilibrium resilience is underestimated for small times t_e for values of C near L_2 (where the upper branch starts). For values of C near L_1 , the resilience $\mathcal{R}(t_e)$ is very small but has already converged for small time t_e . These results show that each of the saddle-node bifurcations has quite a different effect on the conditional resilience of the background states on the upper and lower branch.

3.3. Time-dependent C case

As an illustrative function $C(t)$ describing the change in pCO₂, we choose

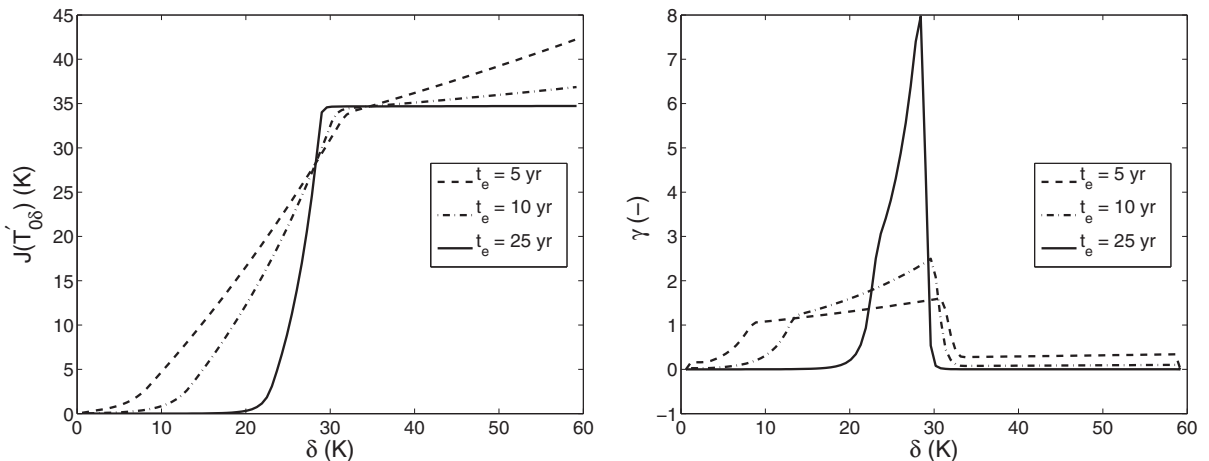


Fig. 3. (a) Values of $J(T'_{0\delta})$ for four different values of t_e . (b) Values of the slope $\gamma = \partial J(T'_{0\delta})/\partial \delta$ in (a).

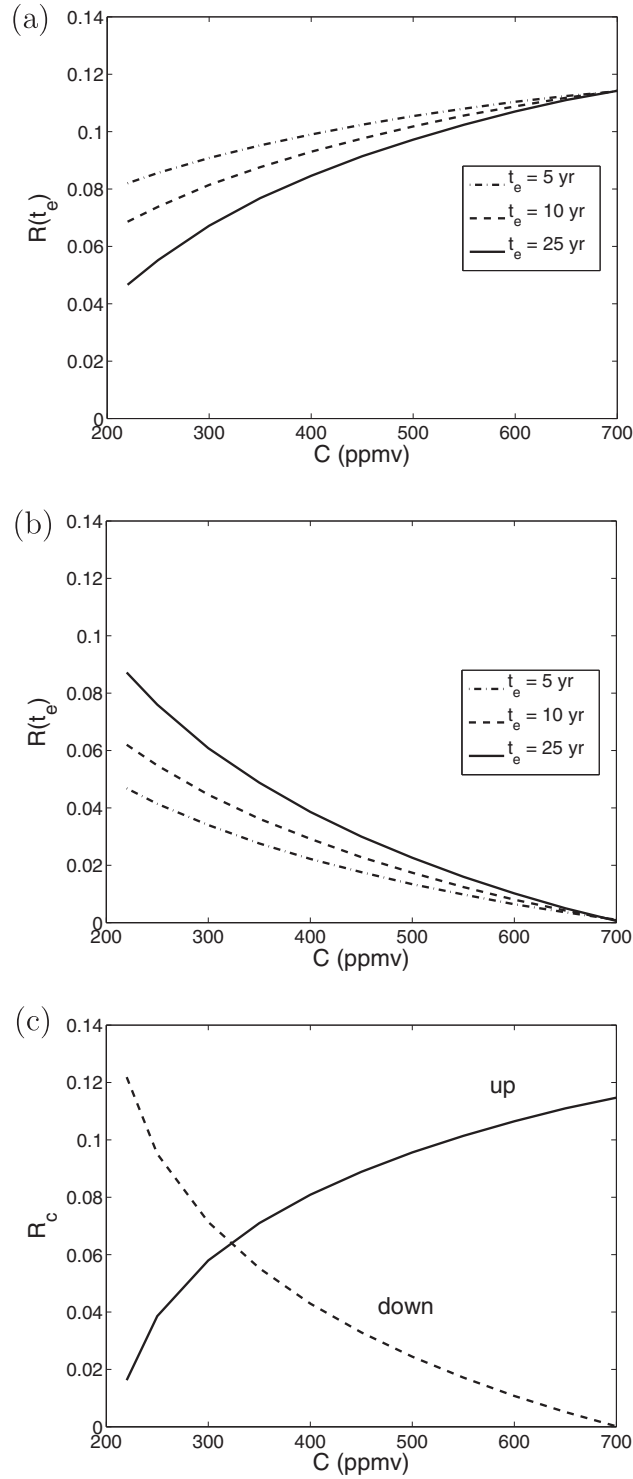


Fig. 4. (a–b) Values of $\mathcal{R}(t_e)$ for different times t_e for each background state along (a) the upper branch and (b) the lower branch in Fig. 2. (c) Values of \mathcal{R}_c along upper and lower branch of the bifurcation diagram in Fig. 2.

$$C(t) = C_1 + (C_2 - C_1) \tanh\left(\frac{t}{\tau_f}\right). \quad (16)$$

This represents an increasing value of C , starting at C_1 for $t = 0$ and equilibrating on a time scale τ_f to a new value C_2 . With $C_1 = C_0$, the equilibrium climate sensitivity S_{eq} is determined from

$$S_{eq} = \frac{\Delta T}{\Delta R} \quad (17)$$

where $\Delta C = C_2 - C_1$ and ΔR is related to ΔC through the relation $R = G + A \ln(C/C_0)$ according to (12).

For $C_1 = 300$ ppmv and $C_2 = 600$ ppmv, $t_f = 100$ years, the conditional sensitivity $S(\delta, t_e)$ defined in (11) of the background state ($\bar{C} = 300$ ppmv, $\bar{T} = 294.208$ K) is for several values of t_e plotted versus (relatively small) δ in Fig. 5(a). The equilibrium sensitivity $S_{eq} = 0.17$ K/(W m²) is also shown in Fig. 5(a) (curve for $t_e = 100$ years). For short times t_e the conditional climate sensitivity is substantially larger than the equilibrium values as the warming occurs over a relatively short time period. This is related to the shape of the C curve used. For longer times, the equilibrium climate sensitivity is approached which is independent of δ .

The conditional climate sensitivity is also suited for situations in which bifurcations do occur. For example, suppose we are on the lower branch in a background state is given by $\bar{C} = 300$ ppmv, $\bar{T} = 258.694$ K. When increasing C up to 600 ppmv, the equilibrium climate sensitivity is given by $S_{eq} = 0.249$ K/(W m²). This value is found in Fig. 5(b), for $t_e = 100$ years when δ is relatively small (dotted curve). When the initial perturbations are large, however, the system may jump to another state, increasing the sensitivity greatly. For $t_e = 100$ year, this is seen as a jump in $S(\delta, t_e)$ in Fig. 5(b). For smaller times t_e , it is interesting that the increase in $S(\delta, t_e)$ is seen for larger δ indicating a large transient sensitivity because of the presence of the equilibrium states on the upper branch. Such behavior in $S(\delta, t_e)$ will also occur on the upper branch for larger δ (cf. Fig. 5(a)).

4. Summary and discussion

In this paper, we have suggested the new concepts of conditional climate resilience and conditional climate sensitivity as measures of the nonlinear response of the climate system to finite amplitude perturbations. This was done by framing the issue of the response of the nonlinear system to finite amplitude perturbations as a Conditional Nonlinear Optimal Perturbation (CNOP) problem. The magnitude of the perturbation is related to a norm of the state vector, and the crossing of the attraction basin with a threshold in that norm. One can determine this threshold directly from the CNOP approach because a (well chosen) cost function will generally undergo a sharp transition once the amplitude of the perturbation is increased (and an attraction basin boundary is crossed).

Although the CNOP is only one single perturbation it has the very special property that the distance between the trajectory at time t_e and the reference state is maximal in the chosen norm (under the constraint condition defined by δ). Of course, the choice of the norm, the value of δ and the time t_e are crucial and should be strongly motivated by the specific problem to be meaningful. One could, in principle, also probe the stability of the system using several CNOPs by choosing different norms and constraint conditions. However, for addressing conditional resilience and sensitivity in the climate system, there are already good choices available for the norm (the global mean surface temperature), for the constraint condition (internal variability) and for the evolution time (time scale of interest in climate change, say 10–100 years). These are exactly the quantities in which equilibrium climate sensitivity has been traditionally formulated [1,2].

The conditional climate sensitivity $S(\delta, t_e)$ measures the maximal global mean surface temperature difference (with respect to a background state) which can be realized over a time t_e under initial perturbations with an initial amplitude constraint set by the value of δ . The constraint condition connects the sensitivity to the internal variability: in a background state with large internal variability (large δ) a larger temperature difference may be achieved under a time t_e than in a background

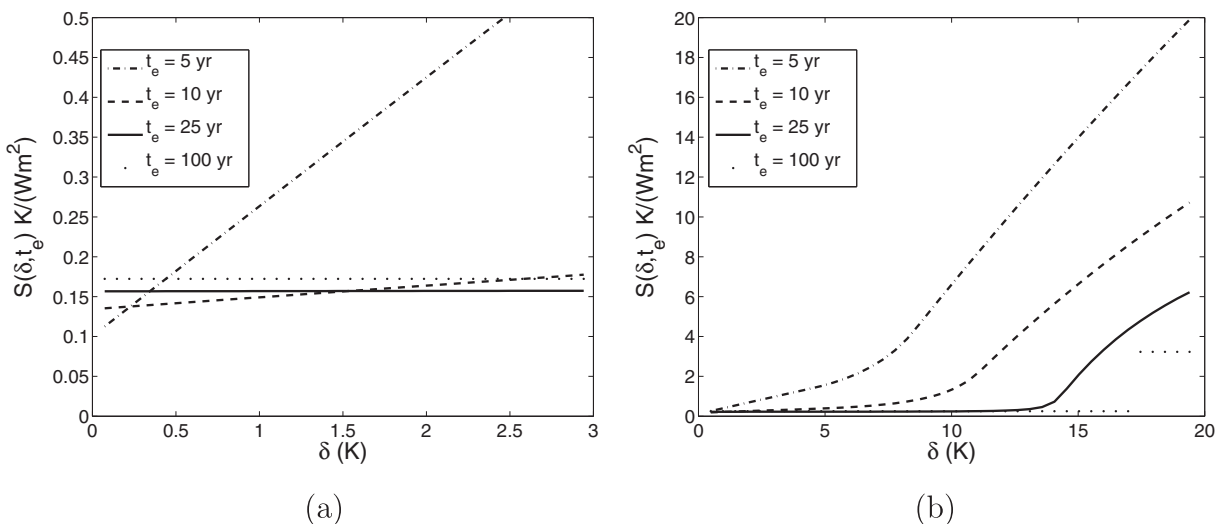


Fig. 5. (a) Values of $S(\delta)$ versus δ for the background state defined as $\bar{C} = 300$ ppmv, $\bar{T} = 294.208$ K. (b) Same as (a) but now for the background state $\bar{C} = 300$ ppmv, $\bar{T} = 258.694$ K.

state with smaller internal variability. In the limit $t_e \rightarrow \infty$, the conditional climate sensitivity approaches the equilibrium climate sensitivity S_{eq} .

The conditional resilience $\mathcal{R}(t_e)$ indicates the degree to which a system is vulnerable to finite amplitude perturbations by determining a measure of the critical boundary (in perturbation amplitude) for which transitions would occur. As discussed in [17], resilience actually has several aspects and they refer to these as ‘latitude’, ‘resistance’, ‘precariousness’ and ‘panarchy’. With the concept of conditional resilience, we only address the first three of these properties; the panarchy (multi-scale interaction) property is out of the scope of this analysis. The ‘latitude’ of resilience is here directly related to the equilibrium resilience \mathcal{R}_e , the ‘resistance’ and ‘precariousness’ is measured by the conditional resilience $\mathcal{R}(t_e)$. Here the absolute value of the conditional resilience reflects the ‘precariousness’ and the change of $\mathcal{R}(t_e)$ with time t_e is a measure for the ‘resistance’.

There is an additional issue to resilience related to the control needed to bring the system back into the original regime of behavior; in [17] this is referred to as adaptability. This issue is mostly involved with how for example fixed points and/or the attraction basins change with the parameters in the problem. In general, it is easier to influence the parameters in the system (which may be only a few) than components of a large-dimensional state vector. This issue is more closely related to control theory (either on the state vector or on the parameters) and outside the scope of this study.

We have illustrated both novel concepts using an idealized zero-dimensional energy balance model. Here the situation is relatively simple with two saddle-nodes bounding a multiple equilibrium regime with two stable fixed points and one unstable fixed point. In the autonomous case (fixed C), the equilibrium conditional resilience was here easily connected to the scalar distance between each stable and unstable state. The conditional resilience itself is dependent on t_e and indicates that for finite time it displays quite different behavior with t_e for cold and warm states in the model. We have also shown that conditional climate sensitivity can deal with systems in which there are multiple equilibria and that relatively large changes in $S(\delta, t_e)$ for small times t_e may provide signatures of the presence of other equilibria.

The energy balance model used here is strongly oversimplified in terms of its dynamical behavior and as a representation of the processes controlling the global mean surface temperature. To generalize the approach to more sophisticated (and spatially extended) climate models, there are several different obstacles which have to be overcome.

1. *The generalization from low-dimensional to high-dimensional dynamical systems, the latter still having relatively simple behavior (fixed points and smooth basin boundaries).* The central computational issue is whether one can compute CNOPs in these higher-dimensional systems. At the moment, this has already been accomplished for quasi-geostrophic [26] and shallow-water models [15] of the wind-driven ocean circulation and full 3D primitive equation models of the thermohaline ocean circulation [27]. Also in the theory of nonlinear stability of fluid flows, there are already many applications of this approach, such as pipe flows [13]. However, it is still a computational challenge to determine a CNOP for a global climate model. Recently, an ensemble method has been proposed to determine CNOPs [28] which can be promising to address this challenge.
2. *The generalization from geometrically simple to complicated (fractal) basin boundaries.* This is an interesting but difficult issue as fractal boundaries can be very complicated geometrical features [29]. When there is a fractal boundary it is not guaranteed anymore that there is a global maximum in the function $\delta(t_e)$ as defined in (9) and other techniques (such as performing large ensemble computations) are needed to assess the resilience of a conditionally stable fixed point.
3. *The generalization from deterministic to stochastic systems.* In one-dimensional systems, such as the conceptual climate model in this paper with noise added, one might address the problem of resilience by using the Fokker–Planck equation associated with the stochastic model. Here, a CNOP for a norm of the probability density function (such as the variance) can be used to define the initial probability density function which will lead to optimal variance at a certain time t_e . In a bimodal system, this can then be used to determine the probability to induce a switch between two invariant measures. For higher-dimensional systems, the Fokker–Planck approach is not feasible and one option may be to apply path-integral methods [30].

The exploration of all of these generalizations needs further investigation before the success of the CNOP approach presented here to obtain a useful measure of climate resilience can be assessed. However, when successful, it opens up a new path towards studying the resilience of the climate system and the effect of its hierarchical organization on this property.

Acknowledgements

We thank the organizers of the workshop “Tipping points: fundamentals and applications” from 9–13 September 2013 at the International Center for Mathematical Sciences at Edinburgh (UK), where most of these ideas were generated. The research was supported by the Netherlands Organization for Scientific Research (NWO) through the COMPLEXITY project PreKurs.

References

- [1] IPCC, 2013, Climate Change 2013: The physical science basis, in: T.F. Stocker, et al. (Eds), Contribution of Working Group I to the Fifth Assessment Report of the Intergovernmental Panel on Climate Change (IPCC), Cambridge University Press, Cambridge, UK and New York, NY, 2013. Available from <www.ipcc.ch>.

- [2] Rohling E, Sluys A, Dijkstra HA, Von der Heydt AS, Köhler P, Van de Wal R. and the PALAEOSENSE team, Making sense of palaeoclimate sensitivity. *Nature* 2013;491(7426):683–91.
- [3] Charney JG. *Carbon Dioxide and Climate: A Scientific Assessment*. Washington DC: National Academy of Science; 1979.
- [4] Knutti R. The equilibrium sensitivity of the Earth's temperature to radiation changes. *Nature Geosci.* 2008;1:735–43.
- [5] Pierrehumbert RT. *Principles of Planetary Climate*. Cambridge, UK and New York, NY: Cambridge University Press; 2012.
- [6] Roe GH, Baker MB. Why is climate sensitivity so unpredictable? *Science* 2007;318(5850):629–32.
- [7] Zaliapin I, Ghil M. Another look at climate sensitivity. *Nonlinear Process. Geophys.* 2010;17(2):113–22.
- [8] Ghil M. A mathematical theory of climate sensitivity. *World Sci. Res.* 2013;1:735–43.
- [9] Thurnburn J. Climate sensitivities via a Fokker–Planck adjoint approach. *Q. J. R. Meteorol. Soc.* 2005;131(605):73–92.
- [10] F. Ragone, V. Lucarini, F. Lunkeit, A new framework for climate sensitivity and prediction, arXiv: 1403.4908.
- [11] Joseph DD. *Stability of Fluid Motions*. Berlin-Heidelberg, Germany: Springer-Verlag; 1976.
- [12] Mu M, Duan W. Conditional nonlinear optimal perturbation and its applications. *Nonlinear Process. Geophys.* 2003;2003:493–501.
- [13] Kerswell RR. Recent progress in understanding the transition to turbulence in a pipe. *Nonlinearity* 2005;18(6):R17–44.
- [14] Pringle CCT, Kerswell RR. Using nonlinear transient growth to construct the minimal seed for shear flow turbulence. *Phys. Rev. Lett.* 2010;105(15):154502.
- [15] Wang Q, Mu M, Dijkstra HA. The similarity between optimal precursor and optimally growing initial error in prediction of Kuroshio large meander and its application to targeted observation. *J. Geophys. Res. Oceans* 2013;118(2):869–84.
- [16] Holling CS. Resilience and stability of ecological systems. *Ann. Rev. Ecol. Syst.* 1973:1–23.
- [17] B. Walker, C.S. Hollin, S.R. Carpenter, A. Kinzig, Resilience, adaptability and transformability in social-ecological systems, *Ecology and Society* 2004;9(2).
- [18] Walker B, Salt D. *Resilience Thinking*. Washington DC: Island Press; 2006.
- [19] Farrell BF, Ioannou PJ. Generalized stability theory: part I: autonomous operators. *J. Atmos. Sci.* 1996;53:2025–40.
- [20] Mu M. Nonlinear singular vectors and nonlinear singular values. *Sci. China Ser. D-Earth Sci.* 2000;43:375–85.
- [21] Mu M, Liang S, Dijkstra HA. The sensitivity and stability of the ocean's thermohaline circulation to finite amplitude perturbations. *J. Phys. Oceanogr.* 2004;34:2305–15.
- [22] Budyko MI. The effect of solar radiations on the climate on the Earth. *Tellus* 1969;21:611–9.
- [23] Sellers WD. A global climate model based on the energy balance of the earth-atmosphere system. *J. Appl. Meteorol.* 1969;8:392–400.
- [24] Hogg AM. Glacial cycles and carbon dioxide: a conceptual model. *Geophys. Res. Lett.* 2008;35(1):L01701.
- [25] Ghil M, Childress S. *Topics in Geophysical Fluid Dynamics: Atmospheric Dynamics, Dynamo Theory, and Climate Dynamics*. Berlin/Heidelberg/New York: Springer-Verlag; 1987.
- [26] van Scheltinga ADT, Dijkstra HA. Conditional nonlinear optimal perturbations of the double-gyre ocean circulation. *Nonlinear Process. Geophys.* 2008;15(5):727–34.
- [27] Zu Z, Mu M, Dijkstra HA. Optimal nonlinear excitation of decadal variability of the North Atlantic thermohaline circulation. *Chin. J. Oceanol. Limnol.* 2013;31(6):1368–74.
- [28] Yin X, Wang B, Liu J, Tan X. Evaluation of conditional non-linear optimal perturbation obtained by an ensemble-based approach using the Lorenz-63 model. *Tellus Ser. A-Dyn. Meteorol. Oceanogr.* 2014;66:373.
- [29] McDonald SW, Grebogi C, Ott E, Yorke JA. Fractal basin boundaries. *Phys. D-Nonlinear Phenom.* 1985;17(2):125–53.
- [30] Navarra A, Tribbia J, Conti G. The path integral formulation of climate dynamics. *PLoS ONE* 2013;8(6):e67022.